

Electronic screening and damping in magnetars

Rishi Sharma, Sanjay Reddy¹

¹*Theoretical Division, Los Alamos National Laboratory, Los Alamos, New Mexico 87545, USA*

We calculate the screening of the ion-ion potential due to electrons in the presence of a large background magnetic field, at densities of relevance to neutron star crusts. Using the standard approach to incorporate electron screening through the one-loop polarization function, we show that the magnetic field produces important corrections both at short and long distances. In extreme fields, realized in highly magnetized neutron stars called magnetars, electrons occupy only the lowest Landau levels in the relatively low density region of the crust. Here our results show that the screening length for Coulomb interactions between ions can be smaller than the inter-ion spacing. More interestingly, we find that the screening is anisotropic and the screened potential between two static charges exhibits long range Friedel oscillations parallel to the magnetic field. This long-range oscillatory behavior is likely to affect the lattice structure of ions, and can possibly create rod-like structures in the magnetar crusts. We also calculate the imaginary part of the electron polarization function which determines the spectrum of electron-hole excitations and plays a role in damping lattice phonon excitations. We demonstrate that even for modest magnetic fields this damping is highly anisotropic and will likely lead to anisotropic phonon heat transport in the outer neutron star crust.

PACS numbers: 97.60.Jd, 63.20.kd, 71.70.Di

Keywords: neutron stars, magnetic fields, Friedel oscillations

I. INTRODUCTION

Highly magnetized neutron stars called magnetars that feature extreme magnetic fields (B) — as large as 10^{15} G on the surface and perhaps even larger fields inside — have been detected in recent years. Currently there are 13 magnetar candidates which are classified as anomalous x-ray pulsars (AXPs) or soft gamma repeaters (SGRs) (<http://www.physics.mcgill.ca/~pulsar/magnetar/main.html>). Such large magnetic fields can strongly influence the state of matter in neutron stars, especially in the lower density region where the characteristic energy scales associated with the matter fields is small compared to the magnetic “perturbation”. Several decades ago, it was realized that even modest magnetic fields could influence the structure of atoms in the atmospheres of magnetized neutron stars and affect the spectral features of the emitted radiation [1]. At the surface, where electrons are localized around nuclei and the system consists of neutral atoms, large magnetic fields distort the atomic structure resulting in rod-like or cigar shapes elongated parallel to B . (For a recent review see [2].) It was realized quite early that these cigar shaped atoms would bind with each other along the magnetic field direction forming polymer chains, and that these chains would interact in the perpendicular plane, resulting in a condensed phase [3]. More recently the physics of these condensed phases for hydrogen has been analyzed and its implications for neutron atmospheres is discussed in Ref. [4]. Here we will consider the effects of the magnetic fields at higher density, in the crusts of magnetars where the electrons are not localized in atomic states but rather form a degenerate Fermi system. This will be important in determining the structural and transport properties of the magnetar crust. Our finding will have implication for crust oscillations (excited in explosive phenomena such as giant flares) and for heat and electrical transport which are important ingredients in the study of magnetic and thermal evolution of magnetars [5, 6].

In this work we will typically restrict the study to strong fields where only a few Landau levels are occupied and this will necessarily restrict us to relatively low density region in the outer crust of the neutron star. ($\rho \lesssim 10^{10}$ g/cm³ for $B \lesssim 10^{15}$ G.) The key microscopic quantity required to characterize the response in our approach is the polarization function, which is the Fourier transform of the density-density correlation function. The expression for the polarization function for a magnetized electron gas is calculated and is found in agreement with previous work [7]. Our new findings in this work are related to identifying and understanding the implications of the electronic response in strong magnetic fields for neutron star structure and transport. The real part of the electron polarization function is related to the screening of the ion-ion potential in the crust. In an unmagnetized crust, screening is dominated by the usual Debye screening. In neutron stars where the typical magnetic field is small ($B \lesssim 10^{11}$ G), the electron screening length is larger than the inter-ion distance and this implies that the effects of electron screening are usually unimportant in determining the crystal structure and thermodynamics. In contrast, we find that for large fields when only one or a few Landau levels are filled, the screening length can be either much smaller or much larger than in the unmagnetized case depending on the density and magnetic field. At relatively low density the screening is enhanced resulting in a screening length that is generically smaller than the inter-ion distance. Our finding of enhanced screening for large B is not new, this was already noted in early work which explored some its implications for nuclear fusion

reactions [8]. The qualitatively new finding of our work is the realization that the sharp Fermi surface in the electron momentum distribution along the B field will give rise to long-range oscillatory behavior called Friedel oscillations in the ion-ion potential — a well studied feature in the condensed matter context for $B = 0$. The period of this spatial oscillation $\lambda_F = \pi/(k_f^z)$, where k_f^z the Fermi momentum of the electrons in the z -direction, where we have assumed that B is parallel to z . This potential falls off slowly as $1/z$ on a scale of several inter-ion distances and consequently can be very important in determining the phase structure of the crust. We speculate that this will lead to the formation of an anisotropic crystal with rod-like structures akin to the polymer chains expected in the atomic regime.

The imaginary part of the polarization is related to dissipation and gives rise to the usual Landau damping observed in Fermi systems. In the crust of a neutron star, excitations such as lattice phonons couple to the electrons, and their mean free paths are largely determined by the efficiency of the electronic Landau damping where the phonon decays by producing an electron-hole pair. We show that this decay rate has a non-trivial dependence on the angle between their propagation direction and the magnetic field because the electron-hole excitation for large B is highly anisotropic. This anisotropy leads to an anisotropy in heat transport properties of lattice phonons. We find that the lattice phonons can be scattered more easily if they are moving perpendicular to the field, compared to when they are moving parallel to it.

The paper is organized as follows. In Section II we derive the polarization function of electrons in the presence of a magnetic field. In the Sections III and IV, we apply the result to two physical problems. In Section III we present numerical results for Friedel oscillations. In Section IV we discuss the effect of anisotropic polarization on the decay rates of the lattice phonons as a function of the angle between the propagation direction and the magnetic field.

We discuss the implications for the structure of the magnetar crust in Section V. Details of calculations of the expression for the screened potential are given in Appendix A and Appendix B.

II. POLARIZATION OF ELECTRONS IN A MAGNETIC FIELD.

The Lagrangian for the electron gas in an external electromagnetic field and at finite chemical potential μ is given by,

$$L = \int d^3x \bar{\psi} (i\mathcal{D} - m_e + \mu\gamma^0) \psi, \quad (1)$$

where $D_\mu = \partial_\mu - ieA_\mu$ and m_e is the electron mass. We consider a time independent, uniform magnetic field B in the z direction and choose a gauge such that the only non-zero component of the gauge field A is $A^x = -A_x = By$. The spectrum of electron energy levels in an external magnetic field is well known and electrons occupy Landau levels with energies given by

$$E_m = \sqrt{(k_m^z)^2 + 2meB + m_e^2}, \quad (2)$$

where m is the quantum number associated with the Landau level and k_m^z is the momentum in the z direction. The number density of electrons is

$$n_e = \frac{eB}{(2\pi)^2} \left(\int_{-\infty}^{\infty} dk^z f_0 + 2 \sum_{m>0} \int_{-\infty}^{\infty} dk^z f_m \right) \quad (3)$$

where $f_m = (\exp(\frac{E_m - \mu}{T}) + 1)^{-1}$ is the Fermi distribution function. At $T = 0$, we obtain

$$n_e = \frac{eB}{2\pi^2} \left(\sqrt{\mu^2 - m_e^2} + 2 \sum_{m>0} \theta(\mu^2 - m_e^2 - 2meB) \sqrt{\mu^2 - m_e^2 - 2meB} \right). \quad (4)$$

We will often restrict to the low-density or large magnetic field limit, where only the lowest Landau level is occupied. This occurs for $2eB > \mu^2 - m_e^2$.

The density-density correlation function is defined as

$$\chi_B(x^\mu, y^\mu) = \frac{1}{i} \langle T \{ n(x) n(y) \} \rangle, \quad (5)$$

where $n(x) = \psi^\dagger(x)\psi(x)$ is the density operator. The Lagrangian is time independent for a static external field and even though the Lagrangian looks position dependent in a particular gauge, the system itself is translationally

invariant. (The change in the Hamiltonian due to a translation in x can be undone by a gauge transformation.) Therefore we can write the correlation function in momentum space as,

$$\chi_B(x^\mu, y^\mu) = \int \frac{d\omega}{2\pi} \frac{1}{V} \sum_{\mathbf{q}} e^{iq_\mu(x-y)^\mu} \Pi_B(\omega, \mathbf{q}), \quad (6)$$

where $q^\mu = (\omega, \mathbf{q}) = (\omega, q_\perp, q^z)$.

To evaluate Π_B , we insert a complete set of many-body eigenstates between the two density operators in Eq. 5. We ignore the anti-particle contribution to the polarization function because they are well below the Fermi level and retain only particle-hole contributions. In this approximation we can write the polarization as,

$$\begin{aligned} \Pi_B(q^\mu) &= \frac{eB}{2\pi} \sum_{m,n} \int_{-\infty}^{\infty} \frac{dk_m^z}{2\pi} f_m(1-f_n) W(E_m, E_n, m, n, k_m^z, k_n^z, q_\perp) \\ &\quad \left[\frac{1}{\omega - E_n + E_m + i\epsilon} - \frac{1}{\omega + E_n - E_m - i\epsilon} \right] \Big|_{k_n^z = k_m^z + q^z}, \end{aligned} \quad (7)$$

where, m refers to the (initial) energy eigenstate with energy $E_m = \sqrt{(k_m^z)^2 + 2meB + m_e^2}$ and n to the (final) state with energy $E_n = \sqrt{(k_n^z + q^z)^2 + 2neB + m_e^2}$. The function W contains the matrix elements of the density operator between different electron eigenstates and is given by ,

$$\begin{aligned} W = W(E_m, E_n, m, n, k_m^z, k_n^z, q_\perp) &= \frac{1}{2E_n E_m} \left[(E_m E_n + k_m^z k_n^z + m_e^2) H_{m-1, n-1}(q_\perp) H_{m-1, n-1}^*(q_\perp) \right. \\ &\quad + (\sqrt{2meB} \sqrt{2neB}) H_{m-1, n-1}(q_\perp) H_{m, n}^*(q_\perp) \\ &\quad + (\sqrt{2meB} \sqrt{2neB}) H_{m, n}(q_\perp) H_{m-1, n-1}^*(q_\perp) \\ &\quad \left. + (E_m E_n + k_m^z k_n^z + m_e^2) H_{m, n}(q_\perp) H_{m, n}^*(q_\perp) \right], \end{aligned} \quad (8)$$

where,

$$H(q_\perp) = \begin{cases} m \geq n & [e^{-q_\perp^2 l^2/4} \sqrt{\frac{n!}{m!}} \left(\frac{(-q^x - iq^y)l}{\sqrt{2}} \right)^{m-n} L_n^{m-n}(q_\perp^2 l^2/2)] \\ m \leq n & [e^{-q_\perp^2 l^2/4} \sqrt{\frac{m!}{n!}} \left(\frac{(q^x + iq^y)l}{\sqrt{2}} \right)^{n-m} L_m^{n-m}(q_\perp^2 l^2/2)] \end{cases}. \quad (9)$$

Here, $L_a^b(x)$ are the associated Laguerre polynomials, and $l = 1/\sqrt{eB}$ is the magnetic length. For $m = 0$ or $n = 0$, $H_{m-1, n-1}(X) = 0$.

The imaginary and real parts of the response function can be separated by following the pole prescription,

$$\frac{1}{\omega - \Delta E \pm i\epsilon} = \text{P}\left(\frac{1}{\omega - \Delta E}\right) \mp i\pi\delta(\omega - \Delta E). \quad (10)$$

This gives the imaginary part,

$$\begin{aligned} \Im m[\Pi_B(q^\mu)] &= \frac{eB}{2\pi} (-\pi) \sum_{m,n} \int_{-\infty}^{\infty} \frac{dk_m^z}{2\pi} f_m(1-f_n) W(E_m, E_n, m, n, k_m^z, k_n^z, q_\perp) \\ &\quad [\delta(\omega - E_n + E_m) - \delta(\omega + E_n - E_m)] \Big|_{k_n^z = k_m^z + q^z}, \end{aligned} \quad (11)$$

We want to consider situations where the temperature is much less than the chemical potential μ . In this case, it is appropriate to approximate f_m by $\theta(\mu - E_m)$ and $1 - f_n$ by $\theta(E_n - \mu)$.

The real part of Π_B is given by,

$$\begin{aligned} \Re e[\Pi_B(q^\mu)] &= \frac{eB}{2\pi} \sum_{m,n} \int_{-\infty}^{\infty} \frac{dk_m^z}{2\pi} f_m W(E_m, E_n, m, n, k_m^z, k_n^z, q_\perp) \\ &\quad \text{P}\left[\frac{1}{\omega - E_n + E_m} - \frac{1}{\omega + E_n - E_m} \right] \Big|_{k_n^z = k_m^z + q^z}, \end{aligned} \quad (12)$$

In particular, to calculate screening, we will be interested in the static response, $\omega = 0$, which is given by,

$$\begin{aligned} \Re e[\Pi_B(0, \mathbf{q})] &= \frac{eB}{\pi} \sum_{m,n} \int_{-\infty}^{\infty} \frac{dk_m^z}{2\pi} f_m W(E_m, E_n, m, n, k_m^z, k_n^z, q_\perp) \\ &\quad \text{P}\left[\frac{1}{E_m - E_n} \right] \Big|_{k_n^z = k_m^z + q^z}. \end{aligned} \quad (13)$$

In the limit $T = 0$,

$$\Re e[\Pi_B(0, \mathbf{q})] = \frac{eB}{2\pi} 2 \sum_{m,n} \int_{-\infty}^{\infty} \frac{dk_m^z}{2\pi} W(E_m, E_n, m, n, k_m^z, k_n^z, q_{\perp}) \theta(\mu - \sqrt{(k^z)^2 + m_e^2 + 2meB}) \mathcal{P}\left[\frac{1}{E_m - E_n}\right]_{|k_n^z = k_m^z + q^z} . \quad (14)$$

We will now use these results for calculating two important physical processes of relevance to magnetars: (i) the screening of electric charge by the electron gas and the resulting modification of the ion-ion potential in the crust (Section III), and (ii) the anisotropic spectrum of electron-hole excitations (Landau damping) and its consequences for the phonon mean free paths in the outer crust (Section IV).

III. SCREENING IN AN ELECTRON GAS

The screened potential between two ions with charges Z_1 and Z_2 separated by a displacement \mathbf{r} in an electron gas is given by

$$V_{\text{mod}}(\mathbf{r}) = \frac{Z_1 Z_2 e^2}{4\pi r} g(\mathbf{r}),$$

where $g(\mathbf{r}) = 4\pi r \int \frac{d^3 q}{(2\pi)^3} \frac{e^{i\mathbf{q}\cdot\mathbf{r}}}{q^2 + F(\mathbf{q})}$ (15)

gives the modification of the bare interaction due to the polarizability of the electron gas. The function $F(\mathbf{q}) = -e^2 \Re e[\Pi_{00}(\omega = 0, \mathbf{q})]$ is related to the static polarization function of the electron gas, $\Pi_{00}(0, \mathbf{q})$. In evaluating the integral in Eq. 15, typically it is assumed that for distances $r \gtrsim 1/k_f$, where k_f is the Fermi momentum of the electrons, we can replace $\Pi_{00}(0, \mathbf{q})$ by $\Pi_{00}(0, \mathbf{0})$. In doing so one obtains the usual Debye screened potential in coordinate space

$$V_{\text{mod}}(r) = \frac{Z_1 Z_2 e^2}{4\pi r} \exp(-r/\lambda_D), \quad (16)$$

or $g(r) = \exp(-r/\lambda_D)$ where $\lambda_D = 1/\sqrt{F(\mathbf{0})}$ is the Debye screening length, and is simply related to the Debye mass m_D , by $\lambda_D = 1/m_D$. $F(\mathbf{0})$ can be calculated using the well known compressibility sum-rule [9] and is given by

$$F(\mathbf{0}) = e^2 \frac{\partial n_e}{\partial \mu_e}, \quad (17)$$

where n_e is the equilibrium density and μ_e is the chemical potential and $e^2 = 4\pi/137$.

For a free electron gas $F(\mathbf{0}) = e^2 k_f \mu / \pi^2$ with $\mu = (k_f^2 + m_e^2)^{1/2}$. The ion density $n_I = 3/(4\pi a^3)$ — where a is the average inter-particle separation (for a simple cubic crystal a is related to the lattice spacing L by $(4\pi/3)^{1/3} a = L$) — and the electron density are related by electric charge neutrality which requires that $n_e = Z n_I$, where Z is the charge of each ion. Consequently, the electron Fermi momentum k_f and the average inter-ion distance a are related by $k_f = (3\pi^2 Z n_I)^{1/3} = 5.66 (Z_{26})^{1/3} a^{-1}$ where $Z_{26} = Z/26$. Further, from Eq. 17 we have $\lambda_D = 10.37 \sqrt{v_f}/k_f$ where $v_f = k_f/\mu$. The ratio of the screening length to the average inter-ion distance is therefore given by

$$\frac{\lambda_D}{a} \simeq \frac{1.83}{(Z_{26})^{1/3}} \sqrt{v_f}, \quad (18)$$

implying that in the relativistic regime, where $k_f \gg m_e$ and $v_f \simeq 1$, $\lambda_D \simeq 1.83 a$. Since the interaction between the nearest ionic neighbors is essentially unscreened in the relativistic electron gas, screening is not considered to be important for determining the structure of the neutron star crust. This situation is changed if the electrons are non-relativistic. For $Z_{26} = 1$, $\lambda_D < a$ for $v_f < 0.3$. However at lower densities, where $v_f \ll 1$, orbital effects from the localization of electrons may be important and a simple screening approximation is not valid.

Extending the Debye approximation to an electron gas in a magnetic field, setting $F_B(\mathbf{q})$ to its long-wavelength limit $F_B(\mathbf{q} = \mathbf{0})$, we can deduce how the Debye screening is modified by the magnetic field. When only one Landau level is occupied, we find

$$\lambda_D(2eB > \mu_e^2 - m_e^2) = \frac{\pi\sqrt{2}}{e\sqrt{eB}} \sqrt{v_f^z}, \quad (19)$$

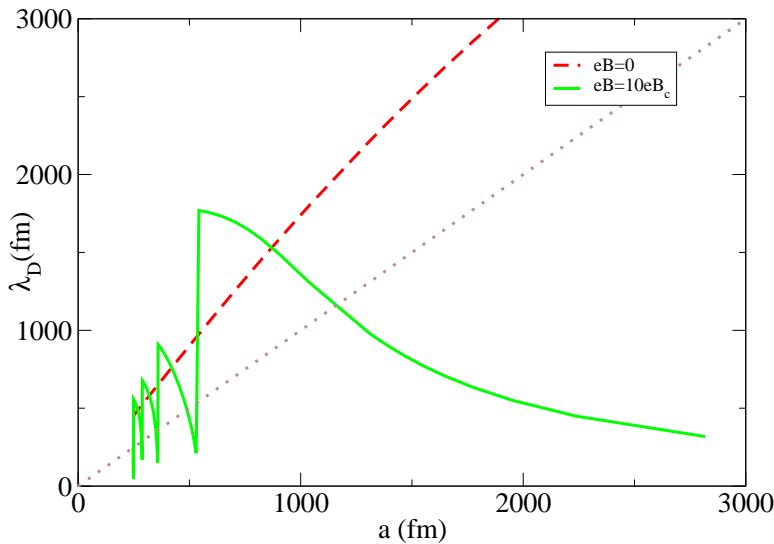


FIG. 1: (color online) The screening length λ_D versus the inter-particle separation a for $Z = 26$ and $eB = 10eB_c$. The dotted line corresponds to $\lambda_D = a$. For $a \gtrsim 512(\text{fm})$, the lowest Landau level is occupied, and for large regions $\lambda_D < a$. As a decreases, more levels are occupied.

which can be smaller or larger than a . Hence the screening length between ions relative to their separation can be tuned arbitrarily by introducing a large magnetic field. To illustrate this we plot λ_D versus a for $eB = 10eB_c$ in Fig. 1. In the low density regime where only one Landau level is filled, $\lambda_D < a$ for $a > 1164(\text{fm})$. With increasing density (smaller a), λ_D becomes larger than a and continues to oscillate around the $B = 0$ value as more Landau levels are occupied. The amplitude of these oscillations rapidly decreases with n where n is the number of Landau levels filled. As noted earlier, for $B = 0$ the screening length is always larger than a when electrons are relativistic.

At low temperatures the Fermi surface of the electrons is sharp and this gives rise to non-analyticities in $F(\mathbf{q})$. Therefore it is not possible to approximate $F(\mathbf{q})$ in Eq. 15 by $F(\mathbf{0})$ even for $r \gg 1/k_f$. The screened potential in position space depends on the polarization function for values of \mathbf{q} other than $\mathbf{q} = \mathbf{0}$, and has qualitative new features compared to the Debye screened result. This phenomenon is well known for the free electron gas ($B = 0$) [9].

Kapusta and Toimela [10] employed the fully relativistic polarization function for electrons at one-loop order to calculate the most general form of the screened potential in a free electron gas. The central result of their calculation is that $F(\mathbf{q})$ has branch cuts along $q = |\mathbf{q}| = \pm 2k_f + i\eta$ for $\eta > 0$. Consequently at large distances, where $r \gg \lambda_D$ the screened potential exhibits characteristic oscillations called Friedel oscillations. It is well established [9] that in the non-relativistic limit the screening function is given by

$$g_{\text{Friedel(NR)}}(r \gg \lambda_D) = \frac{4\xi^2}{(4 + \xi)^2} \frac{\cos(2k_f r)}{(r/\lambda_D)^2}, \quad (20)$$

where $\xi = m_D^2/2k_f^2 = (e^2\mu)/(\pi^2k_f)$. At very low density, where $\xi \gtrsim 1$ Friedel oscillations are non-negligible and have been well studied in condensed matter physics context [9]. The potential between two ions for $r \lesssim \lambda_D$ is dominated by Debye screening. In the region $r \simeq \lambda_D$ a simple analytic form does not exist and the screening function needs to be calculated numerically.

It is also shown in Ref. [10] that in the extreme relativistic limit, when $m_e \rightarrow 0$, Friedel oscillations are modified. At large distances the screening function is of the form

$$g_{\text{Friedel(R)}} = (2\xi)^{3/2} \frac{\sin(2k_f r)}{(r/\lambda_D)^3}. \quad (21)$$

Unlike in the non-relativistic regime, here $\xi = 0.0047 \ll 1$, and amplitude of these oscillations is greatly suppressed. Furthermore they decay as $1/r^3$ instead of $1/r^2$ in the non-relativistic limit. Consequently, Friedel oscillations can be ignored in the relativistic regime.

In the presence of a magnetic field, the screening function $F_B(\mathbf{q})$ is no longer rotationally symmetric and we expect the screened potential to be anisotropic. We now proceed to calculate $V(\mathbf{r})$ in this case. The calculation of the polarization tensor when the densities are high and several Landau levels are occupied, is technically complicated. On the other hand, in this limit one expects the results to be very similar to the free electron gas. Therefore we restrict

ourselves to the large field limit, when only the lowest Landau level is filled. In cylindrical variables we write $F_B(\mathbf{q})$ as a function of $q^z = q \cos \theta$ and $q_\perp = q \sin \theta$, where θ is the angle between the \mathbf{q} and the magnetic field \mathbf{B} . Note that Debye screening — which depends only on $F_B(\mathbf{0})$ — is completely isotropic.

In cylindrical spatial coordinates the potential between two ions

$$V_{\text{mod}}(\rho, z) = \frac{Z_1 Z_2 e^2}{4\pi r} g(\rho, z),$$

$$\text{where } g(\rho, z) = \frac{r}{\pi} \int_0^\infty dq_\perp q_\perp J_0(q_\perp \rho) \int_{-\infty}^\infty dq^z \frac{e^{iq^z z}}{q^2 + F_B(q_\perp, q^z)}, \quad (22)$$

with $r = \sqrt{\rho^2 + z^2}$, $F_B(q_\perp, q^z) = -e^2 \Pi_B(0, \mathbf{q})$, and $\Pi_B(0, \mathbf{q})$ is the static polarizability of the electron gas in the presence of a magnetic field.

Restricting to $m = 0$ in the sum in Eq. 14, we have,

$$F_B(q_\perp, q^z) = e^2 \frac{eB}{2\pi} \sum_n \int_{-\infty}^\infty \frac{dk^z}{2\pi} 2\theta(\mu - \sqrt{(k^z)^2 + m_e^2}) \frac{W(E_0, E_n, m, n, k_0^z, k_n^z, q^z)}{E_n - E_0}. \quad (23)$$

The sum over n in Eq. 23 runs over all non-negative integers, but the most important contribution for $eB \gg \mu^2$ and $eB \gg q^2$ is the $n = 0$ term. (This is shown in Appendix A.) Therefore for simplicity, we drop the $n > 0$ terms, which allows us to calculate analytic expressions for $F_B(\mathbf{q})$, and the screened Coulomb interaction in certain limits. With these approximations,

$$F_B(q_\perp, q^z) \sim \left(\frac{e}{\pi}\right)^2 \left(\frac{eB}{2}\right) e^{-q_\perp^2/(2eB)} \int_{-k_f^z}^{k_f^z} dk^z \frac{1}{\sqrt{(k^z + q^z)^2 + m_e^2} - \sqrt{(k^z)^2 + m_e^2}} \frac{((k^z + q^z)k^z + m_e^2 + \sqrt{(k^z)^2 + m_e^2} \sqrt{(k^z + q^z)^2 + m_e^2})}{2\sqrt{(k^z)^2 + m_e^2} \sqrt{(k^z + q^z)^2 + m_e^2}}, \quad (24)$$

where $k_f^z = \sqrt{\mu^2 - m_e^2}$ is the Fermi momentum of the electrons in the z direction for the $m = 0$ level. If higher levels are occupied, each will have a different Fermi momentum.

Now we consider two limiting cases. First, in the non-relativistic regime where $m_e \gg k_f^z$, we obtain for large B ,

$$F_B(q_\perp, q^z) \sim \left(\frac{e}{\pi}\right)^2 \left(\frac{eB}{2}\right) e^{-q_\perp^2/2eB} \int_{-k_f^z}^{k_f^z} dk^z \left(\frac{m_e}{(k^z + q^z)^2 - (k^z)^2} \right)$$

$$= \left(\frac{e}{\pi}\right)^2 \left(\frac{eB}{2}\right) e^{-q_\perp^2/2eB} \log \left(\frac{2k_f^z + q^z}{2k_f^z - q^z} \right) \frac{m_e}{q^z}. \quad (25)$$

The Debye mass is given by

$$m_D^2 = \lim_{\mathbf{q} \rightarrow \mathbf{0}} F_B(q_\perp, q^z) = \left(\frac{e}{\pi}\right)^2 \left(\frac{eB}{2}\right) \left(\frac{m_e}{k_f^z}\right), \quad (26)$$

and since $n_e = eB/(2\pi^2) \sqrt{\mu^2 - m_e^2}$, the above expression (Eq. 26) is consistent with Eq. 17. The key feature of the expression for $F_B(q_\perp, q^z)$ in Eq. 25 is its non-analytic behavior as a function of q^z . In the complex plane, Eq. 25 has branch cuts along $q^z = \pm 2k_f^z + i\eta$, $\eta > 0$. Restricting q^z to the real axis, one sees a kink at $q^z = \pm 2k_f^z$ (Fig. 2). On the other hand the expression is analytic in q_\perp . Based on this we can expect long range oscillations in $g(z)$ with wavelength π/k_f^z in the z direction, but no long range features in the $x - y$ plane.

In the relativistic regime, where $m_e \ll \mu$ we find that

$$F_B(q_\perp, q^z) \sim \left(\frac{e}{\pi}\right)^2 \left(\frac{eB}{2}\right) e^{-q_\perp^2/2eB} \int_{-k_f^z}^{k_f^z} dk^z \frac{(k^z + q^z)k^z + |k^z||k^z + q^z|}{2|k^z||k^z + q^z|} \left(\frac{1}{-|k^z| + |k^z + q^z|} \right)$$

$$= \begin{cases} \left(\frac{e}{\pi}\right)^2 \left(\frac{eB}{2}\right) e^{-q_\perp^2/2eB} & q_\perp < k_f^z \\ \left(\frac{e}{\pi}\right)^2 \left(\frac{eB}{2}\right) e^{-q_\perp^2/2eB} \frac{k_f^z}{|q^z|} & q_\perp > k_f^z \end{cases}. \quad (27)$$

The debye mass square is $m_D^2 = \lim_{\mathbf{q} \rightarrow \mathbf{0}} F_B(q_\perp, q^z) = \left(\frac{e}{\pi}\right)^2 \left(\frac{eB}{2}\right)$. The number of electrons in these limits is $n_e = eB/(2\pi^2) \sqrt{\mu^2 - m_e^2} \sim (eB/(2\pi^2))\mu$ and therefore $m_D^2 = e^2 dn_e/d\mu_e = e^2(eB/(2\pi^2))$ as expected.

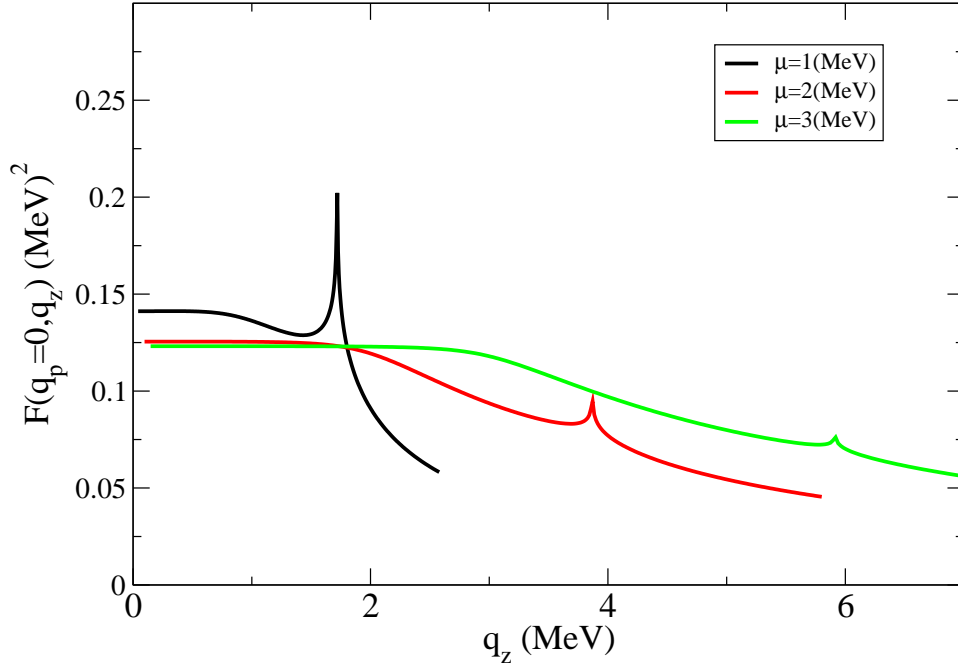


FIG. 2: (color online) F_B as a function of q^z for $q_\perp = 0$, $eB = 100eB_c$, and three values of μ . As the electrons become more relativistic (μ increases), the kink at $2k_f^z$ becomes less sharp. The shoulder at k_f^z becomes non analytic in the ultra-relativistic limit.

From Eq. 27 we note that in the ultra-relativistic limit F_B does not have any non-analytic behavior at $q^z = 2k_f^z$. On the other hand F_B is non-differentiable at $q^z = k_f^z$. This behavior is different from that of a free electron gas, where the non-analyticity occurs at $\pm 2k_f^z$ in both the relativistic and non-relativistic limits. However, this is an artifact of the ultra-relativistic limit, and for any finite m_e , F_B is differentiable at $q^z = k_f^z$. We plot $F_B(q^z)$ for three values of μ in Fig. 2. We notice that for fixed μ there are two distinct features in the plot versus q^z . First, there is shoulder at k_f^z which becomes sharper as m_e/μ decreases. Second, there is a kink at $2k_f^z$ which becomes less prominent as m_e/μ decreases. In the ultra-relativistic limit the kink disappears, and the shoulder becomes a non-differentiable point. However, for any finite m_e , the fact that the kink becomes less prominent suggests that the Friedel oscillations will become weaker as m_e/μ decreases. Hence, we will now focus on the non-relativistic limit.

In the non-relativistic limit, we can obtain an analytic expression for $g(\rho, z)$ valid for $z \gg 1/k_f^z$. We find

$$g(\rho, z) = g_D(\rho, z) + g_F(\rho, z), \quad (28)$$

where,

$$g_D(\rho, z) = e^{-m_D \sqrt{\rho^2 + z^2}} \quad (29)$$

is the Debye screening formula which comes from the pole in the integrand in Eq. 22 at $q = im_D$, and

$$g_F(\rho, z) = -\frac{\sqrt{\rho^2 + z^2} \cos(2k_f^z z)}{\pi} \frac{m_D^2(\pi/4)\rho}{z \sqrt{(2k_f^z)^2 + m_D^2(1/2) \ln(4k_f^z z)}} \times K_1(\rho \sqrt{(2k_f^z)^2 + m_D^2(1/2) \ln(4k_f^z z)}) \quad (30)$$

arises from the branch cuts at $q^z = \pm 2k_f^z + i\eta$. K is a modified Bessel function of the second kind. The derivation of Eq. 28 is given in Appendix B. For $\rho = 0$, we see that $g_F(0, z)$ exhibits long-range Friedel oscillations in the z direction given by

$$g_F(0, z) \sim -\cos(2k_f^z z). \quad (31)$$

Eq. 28 is a good approximation for $z \gtrsim 1/k_f^z$. For $\rho \rightarrow 0$ and $z \rightarrow 0$, we expect that $g(\rho, z)$ should $\rightarrow 1$ since the short range behavior of $V(\mathbf{r})$ can not be modified by screening. For $z \rightarrow 0$ the expression Eq. 28 breaks down because

$(2k_f^z)^2 + m_D^2(1/2) \ln(4k_f^z z) < 0$ but in our derivation we used the fact that $z \gtrsim 1/k_f^z$ and we can not trust Eq. 28 for $z < 1/k_f^z$ anyway. For $\rho = 0$ our derivation remains valid but Eq. 28 can not be used directly since $K_1(a\rho)$ goes as $1/(a\rho)$ as $\rho \rightarrow 0$. The limit of g as $\rho \rightarrow 0$, however, is finite because $a\rho K_1(a\rho)$ tends to 1 as $\rho \rightarrow 0$. Therefore we define,

$$g(\rho = 0, z) = e^{-m_D z} - \frac{\cos(2k_f^z z)}{\pi} \frac{m_D^2(\pi/4)}{(2k_f^z)^2 + m_D^2(1/2) \ln(4k_f^z z)}. \quad (32)$$

For $z = 0$ the value of $g(z)$ is well approximated by the Debye screened value

$$g(\rho, z = 0) = e^{-m_D \rho}. \quad (33)$$

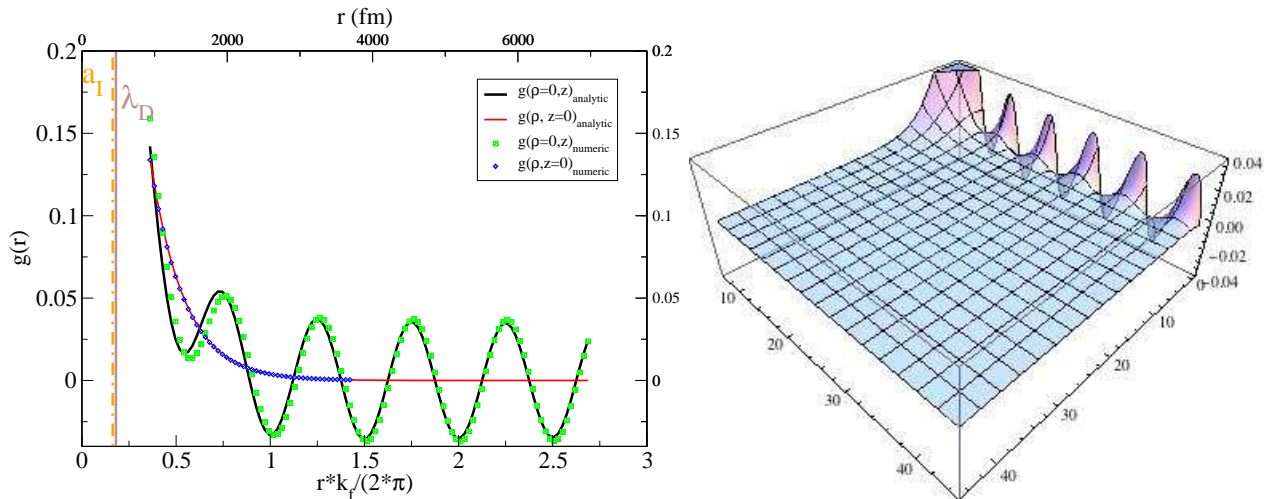


FIG. 3: (color online) Plots of g as a function of ρ for $z = 0$, and as a function of z , for $\rho = 0$ for $eB = 100 eB_c$, $\mu = 0.7$ MeV. g shows an exponential decay as a function of ρ , while along the z axis it shows long range oscillations $\propto -\cos(2k_f^z z)$. Also shown is the Debye screening length λ_D (vertical line, brown online) and $a_I = (3/(4\pi n_I))^{1/3}$ (vertical dot dashed line, orange online, assuming $Z = 26$). The solid lines correspond to the analytic approximations given in Eq. 32 ($\rho = 0$) and Eq. 33 ($z = 0$), while the points correspond to a numerical computation of the Fourier transform in Eq. 15. The right panel shows the 3-d plot of $g(\rho, z)$ in the ρ, z plane with z and ρ .

We have calculated $g(\rho, z)$ for $eB = 100 eB_c$ and $\mu = 0.7$ MeV numerically. For these values, only the lowest Landau level is occupied and the Fermi momentum of the lowest Landau level is $k_f^z = 0.48$ MeV. So the system is mildly relativistic and the electron Fermi energy is large compared to atomic binding energy. The two relevant length scales for the screened potential are the Debye screening length $\lambda_D = 468$ (fm), and the wavelength of Friedel oscillations $\lambda_F = \pi/k_f^z = eB/(2\pi n_e) = 1296$ (fm). In the left panel (Fig. 3) we plot $g(\rho, z)$ along the z and the ρ directions separately. This allows us to see the Friedel oscillations in the z direction clearly, and also compare the numerical results with the approximate analytic expressions. Along the z axis, Eq. 32 is a good approximation to the numerical result, and in the $x - y$ plane, the exponential Debye formula describes the result well. A 3-dimensional plot of $g(\rho, z)$ in the ρ, z plane is shown in the right panel and depicts that the Friedel oscillations are restricted to a narrow cylinder of radius $r \simeq 1/\sqrt{eB}$ in the $x-y$ direction.

For large chosen field of 4.4×10^{15} Gauss, which is near the upper end of what can be found in magnetar surfaces, the amplitude of Friedel oscillations can be very large as shown in Fig. 3. Nonetheless, it is important to note that even small amplitude oscillations can affect the lattice structure due to their long-range character. In our zero temperature treatment the Friedel oscillations are undamped in the z direction due to our assumption of a sharp Fermi surface. A finite temperature will smear the Fermi surface and this will result in exponential damping of Friedel oscillations by the factor $\exp(-z/\xi_T)$, where $\xi_T = 2\pi v_{Fe}/T$ is the thermal correlation length [9] and $v_{Fe} = k_f^z/\mu$ is the Fermi velocity. In neutron stars, the temperature is small and the thermal correlation length $\xi_T \gg a$ where a is the inter-ion distance. Consequently even for small amplitudes, Friedel oscillations can have important effects due to their long-range nature when the screening potential from different ions add coherently.

IV. HEAT TRANSPORT BY LONGITUDINAL LATTICE PHONONS

Lattice phonons (IPhs) are space and time dependent vibrations of the ions, which can transport heat from one region of a solid to another. Typically both longitudinal and transverse modes contribute to heat conduction. In this analysis we restrict ourselves to only longitudinal modes since they primarily couple to electron-hole excitations. At low temperatures, when Umklapp process are suppressed [11], and the occupation numbers of lattice modes is small enough that the non-linear terms in the IPh lagrangian are small, the dominant scattering of IPhs is with the electrons. We first re-derive the relation between the specific heat conductivity of lattice phonons and the imaginary part of the electronic polarization tensor, and recall results for scattering of lattice phonons in a free electron gas. Then we consider scattering in the presence of a magnetic field.

At low temperatures the form of the interaction term between lattice phonons and electrons is well approximated by

$$\mathcal{L}_{el} = -\frac{1}{f_{el}} \int d^3r \psi^\dagger \psi \partial_i \xi^i, \quad (34)$$

where $1/f_{el} = (Ze^2 n_I)/(m_D^2 \sqrt{m_I n_I})$, with n_I , the number density of ions, m_I , the mass of ions, and m_D , the debye screening mass [11].

The rate for phonon decay into an electron-hole ($e-h$) pair can be calculated from the thermal width of the phonon due to absorption by electrons, and is given by the imaginary part of the self energy correction due to the electron loop.

$$\omega \Gamma(q^\mu) = -\frac{q^2}{f_{el}^2} \Im m \Pi(q^\mu), \quad (35)$$

where $\Gamma(q^\mu)$ is the inverse lifetime $1/\tau(q^\mu)$ of the IPh, and $q^\mu = (\omega, \mathbf{q})$. For an on-shell photon $\omega = c_l q$. From Eq. 35, we obtain the mean free path $l_l(q^\mu) = \tau(q^\mu) c_l$,

$$l_l(\omega, \mathbf{q}) = -\left(\frac{c_l^3 f_{el}^2}{\omega \Im m \Pi(\omega, \mathbf{q})}\right), \quad (36)$$

where c_l is the IPh speed.

The thermal conductivity contribution of the lattice phonons from kinetic theory is $\kappa = \frac{1}{3} C_v c_l l_l$. C_v for lattice phonons is simply

$$C_v = \left(\frac{T}{c_l}\right)^3 \left(\frac{2\pi^2}{5}\right). \quad (37)$$

The final expression for the specific heat conductivity for a typical phonon with $\omega = 3T$ is then,

$$\kappa = -\frac{2\pi^2}{15} T^3 \left(\frac{c_l f_{el}^2}{\omega \Im m \Pi(\omega, \mathbf{q})}\right) = -\left(\frac{c_l 2\pi^2 T^2 f_{el}^2}{45 \Im m \Pi(\omega, \mathbf{q})}\right). \quad (38)$$

For $B = 0$ the polarization function (ignoring the antiparticle contribution) of an electron gas is well known [9, 12]. Here, for convenience, we will approximate $\Im m \Pi(q^\mu)$ by its value at $T = 0$. The corrections to this approximation are small if T/μ is small, except at the kinematic boundaries. At $T = 0$ the imaginary part of $\Pi(q^\mu)$ is,

$$\Im m[\Pi(q^\mu)] = -\frac{\mu^2 \omega}{2\pi q} \theta(qv_f - |\omega|). \quad (39)$$

For phonon decay and conductivity in Eq. 38 we are interested in the imaginary part for $\omega/q = c_l < v_f$, which is given by $\Im m[\Pi(q^\mu)] = -\mu^2 c_l/(2\pi)$.

For $B \neq 0$, $\Im m[\Pi_B(q^\mu)]$ is given in Eq. 11. For a representative large value of the field in a magnetar we choose $eB = 10eB_c$, and show results for the imaginary part of the polarization tensor, and the specific heat conductivity κ . The lattice phonons have a typical energy $\omega \sim 3T$, and we take $T = 5\text{keV}$ for our calculation. The magnitude of the momentum is given by $q = \omega/c_s$, and the z and the \perp components are $q \cos \theta$ and $q \sin \theta$ respectively. The speed of lattice phonons depends on the depth, but we take a representative value $c_s \sim 0.05$.

We show the results as a function of the mass density, in commonly used units ρ_{12} corresponding to 10^{12}gm/cc . To convert the mass density, which is dominated by ions, to the electron number density and hence the electron chemical potential, we take the atomic number of ions to be $Z = 26$ and their mass number $A = 56$ (Fe). In Fig. 4, we show

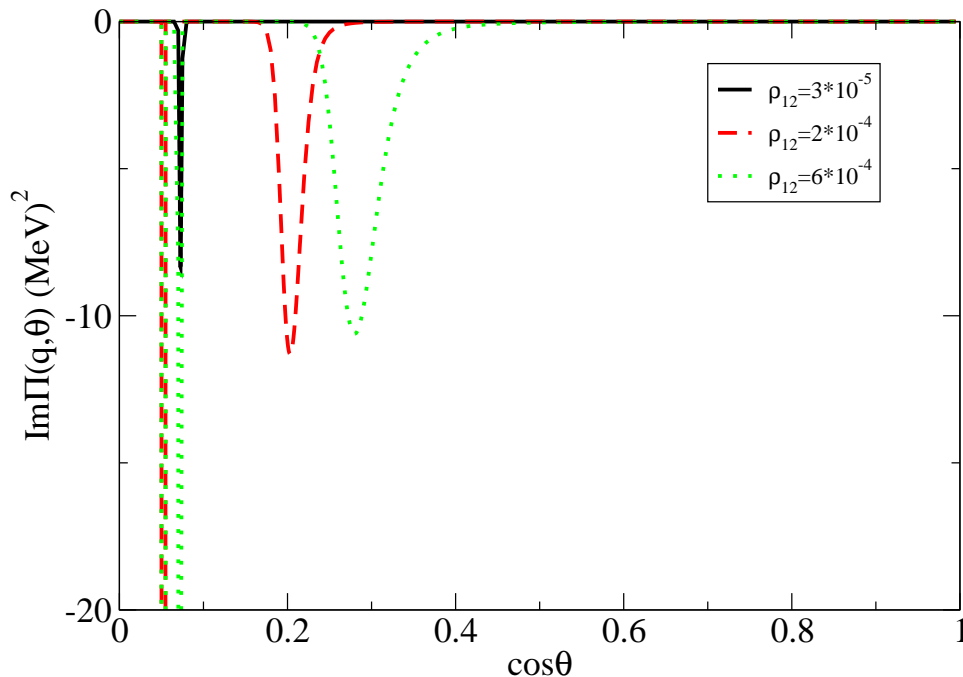


FIG. 4: (color online) A plot of $\Im m[\Pi(\omega = 3T, q_z = \frac{3T}{c_s} \cos \theta, q_\perp = \frac{3T}{c_s} \sin \theta)]$ as a function of the angle θ between the magnetic field and the lPh propagation direction, for three different densities ρ_{12} (10^{12} gm/cc). For this plot $eB = 10eB_c$, $T = 5$ keV, and $c_s = 0.05$. $\cos \theta = 0$ corresponds to a lPh traveling perpendicular to the magnetic field, and $\cos \theta = 1$ corresponds to one traveling parallel to it. At the lowest density, only the lowest Landau level is occupied and scattering is kinematically allowed only at one specific angle. As more levels are occupied, more angles are kinematically allowed.

$\Im m[\Pi_B(q^\mu)]$ as a function of $\cos \theta$ for a three different values of ρ_{12} . In Fig. 5 we show the specific heat conductivity parallel (κ_z) and perpendicular (κ_\perp) to the magnetic field, as a function of ρ_{12} . From Fig. 4 we see that at the lowest densities, the electrons occupy only the lowest Landau levels, and the response is highly anisotropic, and peaked around very specific values of θ , where energy conservation and momentum conservation along the z direction can be simultaneously satisfied. As the density of electrons increases, they occupy higher Landau levels and overall response is obtained by summing contributions from various levels, and is non-zero for several values of θ .

To calculate κ_\perp and κ_z in Fig. 5, we approximate the effective $\Im m[\Pi_B(\omega, \mathbf{q})]$ for scattering parallel to the magnetic field by the average between $\theta = [0, \pi/4]$, and the value perpendicular the magnetic field by the average between $\theta = [\pi/4, \pi/2]$. We see that the lPh conductivity is suppressed perpendicular to the magnetic field but not parallel to it. This result is easy to see in the ultra-relativistic limit. Energy-momentum conservation in this limit requires $|k^z + q \cos \theta| - |k^z| = c_s q$, which can occur only at $\cos \theta = c_s \ll \frac{1}{\sqrt{2}}$. Only at large densities where inter-level transitions become kinematically allowed, does the net response function become relatively isotropic. Formally, κ_z is very large in our calculation, but we have ignored the Umklapp processes which will be important in the z direction, because electron scattering is kinematically suppressed. One can include them by using $\kappa_z^{net} = \kappa_z^e \kappa^U / (\kappa_z^e + \kappa^U)$, where κ_z^e can be read from Fig. 5, and κ^U is the Umklapp contribution. In the perpendicular direction we expect electron scattering to be dominant, and it is alright to ignore the Umklapp contribution.

We note that averaging the response function over angles is a rough method to include the effect of anisotropic scattering. A rigorous procedure will involve solving the transport equation using the anisotropic collision term, that can be deduced from the expression for $\Im m[\Pi_B(q^\mu)]$. We leave such a calculation for future work.

V. CONCLUSIONS

By calculating the one-loop electron-hole polarization function in a strong magnetic field we have found that the screening of the ion-ion potential is significantly different from those obtained in earlier studies where the Debye approximation was assumed. We show for the first time that the Fermi surface of electrons in the direction parallel to the magnetic field leads to Friedel oscillations in the ion-ion potential. These oscillations are large and could fundamentally change the structure of the ionic solid at large field and relatively low density when only the lowest

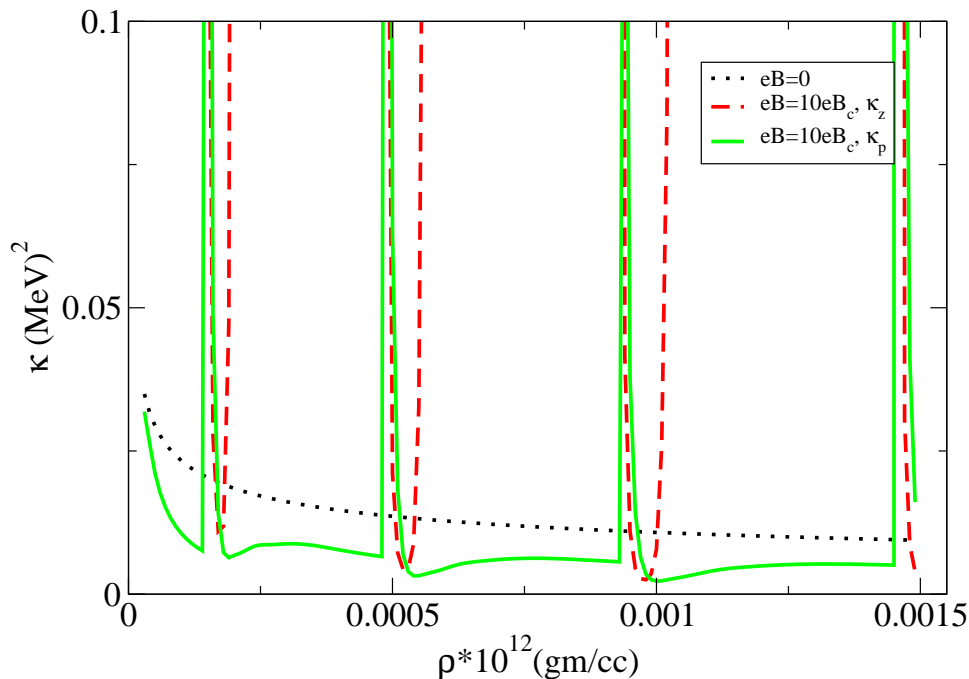


FIG. 5: (color online) Plot of κ as a function of density. κ_z is the specific heat conductivity parallel to the magnetic field, shown by the dashed (red) line. This should be considered as an upper bound for κ_z because our calculation ignores Umklapp processes. κ_\perp is the conductivity perpendicular the field shown by the solid line (green). The dotted line (black) is the conductivity for $B = 0$ at the same density.

Landau levels are occupied. For typical magnetar field strengths of order 10^{15} G, matter up to densities of the order 10^{10} gm/cc will be affected by our finding here. To evaluate how Friedel oscillations and modifications to the average screening length affects the structure and melting properties of the solid we will need to perform either Path Integral Monte Carlo or classical Monte Carlo simulations because the ion-ion interaction is highly non-perturbative. This is beyond the scope of this work and will be investigated separately. Here, we present plausible implications based on qualitative arguments to explore how our findings will modify the ionic structure.

Considering the parameters used in Fig. 3, $eB = 100eB_c$ and $\mu = 0.7(\text{MeV})$ and assuming $Z = 26$, the average number density of ions in the system is $n_I = 3.2 \times 10^{-9} (\text{fm})^{-3}$. If one assumes that the ions form a regular bcc lattice, then the separation between nearest ions is $(\sqrt{3}/2) \times (2/n_I)^{1/3} = 743(\text{fm})$. This is comparable to the screening length λ_D , and smaller than the wavelength for Friedel oscillations λ_F . If significant screening in the $x - y$ plane prevents the formation of a regular bcc structure, it may be favorable to form an anisotropic crystal structure. One possibility is that the ions fit into the troughs in the potential formed by superposition of the $V(z)$ separated in the z axis by λ_F . To maintain neutrality, the ions should arrange themselves in the $x - y$ plane (in a regular or irregular structure) with an average separation $a_\perp = (\pi n_I \lambda_F)^{-1/2} = 278(\text{fm})$.

If indeed the ions in the z direction arrange themselves with separation λ_F , then the following picture arises for the structure of the ion-electron system with changing density, or as we move deeper into the neutron star crust. A single chain of ions arranged along the z axis will look like a rod. $\lambda_F \propto eB/n_I$, and for fixed eB decreases linearly with increasing density. The transverse separation between the rods, $a_\perp \propto (eB)^{1/2}$, on the other hand remains a constant. At the surface, it is known that the elongated atoms form chains parallel to the B field. At low densities (near the surface of the crust), ions will form a plasma of rods with a small charge per unit length (since λ_F is large). These rods will interact with each other by a two dimensional Debye screened Coulomb interaction. As we move deeper into the star, the charge per unit length will keep on increasing, and once λ_F becomes comparable to a_\perp , the system will look more isotropic. This picture will break down when higher Landau levels start being occupied. It is interesting to note that for $Z = 26$, $a_\perp \sim \lambda_F$ implies that $\mu^2 \gtrsim 2eB$, meaning that the next Landau level is occupied. Hence, the point where the screened potential becomes more isotropic coincides with the point where the lattice structure becomes more isotropic. Hence, in our picture, the region where the electrons occupy only the lowest Landau level interpolates smoothly between the surface and the inner crust of the neutron star.

We have also showed that the heat conduction due lattice phonons can become anisotropic because their damping rate due to electron-hole excitations is anisotropic. It is well known that the electronic heat conductivity perpendicular

to the magnetic field is suppressed [13], and this in turn results in a temperature anisotropy at the surface of the neutron star [5]. Our finding that the heat conductivity due to phonons in the direction perpendicular to the magnetic field is also suppressed, is new. This effect may modify the temperature anisotropy in the outer regions of the magnetars during their early thermal evolution.

VI. ACKNOWLEDGEMENTS

We acknowledge discussions with Tanmoy Bhattacharya, Joe Carlson, Stefano Gandolfi and Charles Horowitz. We thank Dima Yakovlev for notes on screening in a magnetic field. RS thanks Huaiyu Duan on discussions about the accurate implementation of Laguerre polynomials.

Appendix A: Dominance of the Lowest Landau level for $eB \gg \mu^2, q^2$

To see that the $n = 0$ term dominates in the sum in Eq. 23, we look at the integrand,

$$\frac{W(E_0, E_n, 0, n, k_m^z, k_n^z, q^z)}{E_m - E_n} = \frac{(E_0 E_n + k_m^z k_n^z + m_e^2) e^{-q^2 l^2 / 2} (q^2 l^2 / 2)^n / n!}{2 E_0 E_n} \frac{1}{E_n - E_m}, \quad (\text{A1})$$

where we have used $L_0^n(x) = 1$. Now, $E_m = \sqrt{(k_m^z)^2 + m_e^2} \sim \mu$. For $n = 0$, $E_n = \sqrt{(k^z + q_\perp)^2 + m_e^2} \sim \mu$ while for $n > 0$, $E_n \sim \sqrt{2neB}$. Therefore, for $n = 0$,

$$\frac{W(E_0, E_n, 0, n, k_m^z, k_n^z, q^z)}{E_n - E_m} \sim e^{-q^2 l^2 / 2} \frac{1}{2\mu}, \quad (\text{A2})$$

while for $n > 0$,

$$\frac{W(E_0, E_n, 0, n, k_m^z, k_n^z, q^z)}{E_n - E_m} \sim \frac{e^{-q^2 l^2 / 2} (q^2 l^2 / 2)^n / n!}{2(E_n - E_m)} \sim \frac{e^{-q^2 l^2 / 2} (q^2 l^2 / 2)^n / n!}{2\sqrt{2neB}}. \quad (\text{A3})$$

Thus, we can conclude that the processes involving excitation to the level n is suppressed compared to the $m = 0$, $n = 0$ transition by a factor $(\mu / (\sqrt{2enB})) (q^2 / (2eB))^n (1/n!)$ which is small if $eB \gg \mu^2$, $eB \gg q^2$.

Appendix B: Derivation of $g(r)$ in the non-relativistic limit

To proceed with the derivation in the non-relativistic limit, we start from the expression,

$$\begin{aligned} g(\rho, z) &= \frac{\sqrt{\rho^2 + z^2}}{\pi} \int_0^\infty dq_\perp q_\perp J_0(q_\perp \rho) \int_{-\infty}^\infty dq^z \frac{\exp(iq^z z)}{(q^z)^2 + q_\perp^2 + F_B(q_\perp, q^z)} \\ &= \frac{\sqrt{\rho^2 + z^2}}{\pi} \int_0^\infty dq_\perp q_\perp J_0(q_\perp \rho) I(q_\perp, z), \end{aligned} \quad (\text{B1})$$

where

$$I(q_\perp, z) = \int_{-\infty}^\infty dq^z \frac{\exp(iq^z z)}{(q^z)^2 + (q_\perp)^2 + F_B(q_\perp, q^z)}. \quad (\text{B2})$$

We calculate the integral $I(q_\perp, z)$ by using contour integration. We assume $z > 0$ and close the contour in the upper half of the complex plane. We have to deform the contour to go around the branch cuts $\pm 2k_f + i\eta$, $\eta > 0$. We call these two parts of the closed contour, C_1 ($q_\perp = 2k_f + i\eta$) and C_2 ($q_\perp = -2k_f + i\eta$). This gives $I(q_\perp, z) + \int_{C_1} dq^z \frac{\exp(iq^z z)}{(q^z)^2 + q_\perp^2 + F_B(q_\perp, q^z)} + \int_{C_2} dq^z \frac{\exp(iq^z z)}{(q^z)^2 + q_\perp^2 + F_B(q_\perp, q^z)} = 2\pi i \text{Res}(\frac{\exp(iq^z z)}{(q^z)^2 + q_\perp^2 + F_B(q_\perp, q^z)})|_{q^z \ni (q^z)^2 + q_\perp^2 + F_B(q_\perp, q^z) = 0}$. We treat these contributions one by one.

First, we look at the pole contribution which we will call the Debye part g_D . The pole is where

$$\begin{aligned} 0 &= q_\perp^2 + (q^z)^2 + F_B(q_\perp, q^z) \\ &= q_\perp^2 + (q^z)^2 + \left(\frac{e}{\pi}\right)^2 \left(\frac{eB}{2}\right) e^{-q_\perp^2 l^2 / 2} \log\left(\frac{2k_f + q^z}{2k_f - q^z}\right) \frac{m_e}{q^z} \end{aligned} \quad (\text{B3})$$

If we assume that the dominant contributions comes from $q^z \ll 2k_f$, then we want

$$\begin{aligned} 0 &= q_{\perp}^2 + (q^z)^2 + \left(\frac{e}{\pi}\right)^2 \left(\frac{eB}{2}\right) e^{-q_{\perp}^2 l^2 / 2} \frac{m_e}{k_f} \\ &= q_{\perp}^2 + (q^z)^2 + m_D^2 e^{-q_{\perp}^2 l^2 / 2} \end{aligned} \quad (B4)$$

This gives, $q^z = i\sqrt{q_{\perp}^2 + m_D^2 \exp(-q_{\perp}^2/(2eB))}$, where we consider the pole in the upper half complex plane. Furthermore if the values of q_{\perp} that contribute strongly to the dq_{\perp} integral are $q_{\perp} \ll \sqrt{2eB}$, we can approximate $\exp(-q_{\perp}^2/(2eB))$ by 1 and

$$\begin{aligned} I_D(q_{\perp}, z) &= 2\pi i \text{Res}\left(\frac{\exp(iq^z z)}{(q^z)^2 + q_{\perp}^2 + m_D^2}\right) \\ &= \frac{2\pi e^{-z\sqrt{q_{\perp}^2 + m_D^2}}}{2\sqrt{q_{\perp}^2 + m_D^2}} \end{aligned} \quad (B5)$$

This is exactly what we obtain if we replace $F(q_{\perp}, q^z)$ by m_D^2 in the first place. Hence, this integral is the same as what we obtain if we assume that there is a simple Debye like screening, and therefore gives,

$$g_D(\rho, z) = e^{-m_D \sqrt{\rho^2 + z^2}} \quad (B6)$$

This is the answer if $q_{\perp} \ll k_f$, \sqrt{eB} dominates the q_{\perp} integral, and if $(\frac{e}{\pi})^2 (\frac{eB}{2})(m_e/k_f) \ll k_f^2$.

Now we consider the integrals over the contours C_1 and C_2 ,

$$\begin{aligned} I_F(q_{\perp}, z) &= \int_{C_1} dq^z \frac{e^{(iq^z z)}}{(q^z)^2 + q_{\perp}^2 + F_B(q_{\perp}, q^z)} + \int_{C_2} dq^z \frac{e^{(iq^z z)}}{(q^z)^2 + q_{\perp}^2 + F_B(q_{\perp}, q^z)} \\ &= \Re e \left[\int_{C_1} dq^z \frac{2e^{(iq^z z)}}{(q^z)^2 + q_{\perp}^2 + F_B(q_{\perp}, q^z)} \right] \\ &= \Re e \left[\int_{-\infty}^0 d\eta \ 2ie^{(2ik_f - \eta)z} \left(\frac{1}{q_{\perp}^2 + (2k_f + i\eta)^2 + (e/\pi)^2 (eB/2)(m/(2k_f + i\eta)) \exp(-q_{\perp}^2/(2eB))(1/2)(\ln((4k_f + i\eta)^2/\eta^2) - i\pi)} \right. \right. \\ &\quad \left. \left. - \frac{1}{q_{\perp}^2 + (2k_f + i\eta)^2 + (e/\pi)^2 (eB/2)(m/(2k_f + i\eta)) \exp(-q_{\perp}^2/(2eB))(1/2)(\ln((4k_f + i\eta)^2/\eta^2) + i\pi)} \right) \right] \\ &= \Re e \left[\int_0^{\infty} d\eta \ 2ie^{(2ik_f - \eta)z} \left(\frac{-1}{q_{\perp}^2 + (2k_f + i\eta)^2 + m_D^2 (k_f/(2k_f + i\eta)) \exp(-q_{\perp}^2/(2eB))(1/2)(\ln((4k_f + i\eta)^2/\eta^2) - i\pi)} \right. \right. \\ &\quad \left. \left. + \frac{1}{q_{\perp}^2 + (2k_f + i\eta)^2 + m_D^2 (k_f/(2k_f + i\eta)) \exp(-q_{\perp}^2/(2eB))(1/2)(\ln((4k_f + i\eta)^2/\eta^2) + i\pi)} \right) \right]. \end{aligned} \quad (B7)$$

Because of the $\exp(-\eta z)$ in the integration over η , for $z \gg 1/k_f$ the integral is dominated by $\eta \sim 1/z \ll k_f$. Therefore we can ignore η whenever it is added to k_f . This simplifies the integral somewhat,

$$\begin{aligned} I_F(q_{\perp}, z) &\sim \Re e \left[\int_0^{\infty} d\eta \right. \\ &\quad \left. \frac{2e^{(2ik_f - \eta)z} m_D^2 \exp(-q_{\perp}^2/(2eB))(\pi/4)}{(q_{\perp}^2 + (2k_f)^2 + m_D^2 \exp(-q_{\perp}^2/(2eB))(1/2) \ln(4k_f/\eta))^2 + (m_D^2 \exp(-q_{\perp}^2/(2eB))(\pi/4))^2} \right]. \end{aligned} \quad (B8)$$

To obtain an analytic form, we need one more simplification. We replace η in $\ln(4k_f/\eta)$ by the value where we expect the integral to dominate, namely $\eta \sim 1/z$. The integral over η can then be evaluated simply, and

$$I_F(q_{\perp}, z) \sim \left[\frac{1}{z} \frac{2 \cos(2k_f z) m_D^2 \exp(-q_{\perp}^2/(2eB))(\pi/4)}{(q_{\perp}^2 + (2k_f)^2 + m_D^2 \exp(-q_{\perp}^2/(2eB))(1/2) \ln(4k_f z))^2 + (m_D^2 \exp(-q_{\perp}^2/(2eB))(\pi/4))^2} \right]. \quad (B9)$$

The Friedel contribution to g is then,

$$\begin{aligned}
g_F(\rho, z) &= -\sqrt{\rho^2 + z^2} \frac{1}{\pi} \int_0^\infty dq_\perp q_\perp J(q_\perp \rho) I_F(q_\perp, z) \\
&= -\sqrt{\rho^2 + z^2} \frac{1}{\pi} \frac{2 \cos(2k_f z)}{z} \int_0^\infty dq_\perp q_\perp J(q_\perp \rho) \\
&\quad \frac{m_D^2 \exp(-q_\perp^2/(2eB))(\pi/4)}{(q_\perp^2 + (2k_f)^2 + m_D^2 \exp(-q_\perp^2/(2eB)))(1/2) \ln(4k_f z)^2 + (m_D^2 \exp(-q_\perp^2/(2eB))(\pi/4))^2}
\end{aligned} \tag{B10}$$

Once again assuming $q_\perp \ll \sqrt{eB}$ we ignore the $\exp(-q_\perp^2/(2eB))$ term as before. Finally, assuming $k_f \gg m_D$ we can drop the $(m_D^2 \pi/4)$ term in the denominator, and

$$\begin{aligned}
g_F(\rho, z) &\sim -\sqrt{\rho^2 + z^2} \frac{1}{\pi} \frac{2 \cos(2k_f z)}{z} \int_0^\infty dq_\perp q_\perp J(q_\perp \rho) \frac{m_D^2(\pi/4)}{(q_\perp^2 + (2k_f)^2 + m_D^2(1/2) \ln(4k_f z))^2} \\
&= -\frac{\sqrt{\rho^2 + z^2} \cos(2k_f z)}{\pi} \frac{m_D^2(\pi/4)\rho}{z \sqrt{(2k_f)^2 + m_D^2(1/2) \ln(4k_f z)}} K_1(\rho \sqrt{(2k_f)^2 + m_D^2(1/2) \ln(4k_f z)}).
\end{aligned} \tag{B11}$$

These manipulations work only if $z \gg 1/k_f$, (long distances in z) and $\rho \ll 1/k_f$. The assumption $\rho \ll 1/k_f$ is not a very essential one because for $\rho \gtrsim 1/k_f$, $g_F(\rho, z)$ decreases very rapidly and this is captured by the expression in Eq. B11, because of the modified Bessel function, K_1 .

Thus, the final answer for large z is,

$$\begin{aligned}
g(\rho, z) &= g_D(\rho, z) + g_F(\rho, z) \\
&= e^{-m_D \sqrt{\rho^2 + z^2}} \\
&\quad - \frac{\sqrt{\rho^2 + z^2} \cos(2k_f z)}{\pi} \frac{m_D^2(\pi/4)\rho}{z \sqrt{(2k_f)^2 + m_D^2(1/2) \ln(4k_f z)}} K_1(\rho \sqrt{(2k_f)^2 + m_D^2(1/2) \ln(4k_f z)}).
\end{aligned} \tag{B12}$$

-
- [1] M. Ruderman, in *Physics of Dense Matter*, edited by C. J. Hansen (1974), vol. 53 of *IAU Symposium*, pp. 117–+.
- [2] H. Ruder, G. Wunner, H. Herold, and F. Geyer, *Atoms in Strong Magnetic Fields. Quantum Mechanical Treatment and Applications in Astrophysics and Quantum Chaos* (Springer-Berlin, 1994).
- [3] M. Ruderman, *Physical Review Letters* **27**, 1306 (1971).
- [4] D. Lai and E. E. Salpeter, *ApJ* **491**, 270 (1997), arXiv:astro-ph/9704130.
- [5] U. Geppert, M. Küker, and D. Page, *A&A* **426**, 267 (2004), arXiv:astro-ph/0403441.
- [6] D. N. Aguilera, J. A. Pons, and J. A. Miralles, *A&A* **486**, 255 (2008), URL <http://dx.doi.org/10.1051/0004-6361:20078786>.
- [7] U. H. Danielsson and D. Grasso, *Phys. Rev. D* **52**, 2533 (1995).
- [8] D. A. Shalybkov and D. G. Yakovlev, *Astrophysics* **27**, 562 (1987).
- [9] A. L. Fetter and J. D. Walecka, *Quantum theory of many-particle systems* (Quantum theory of many-particle systems, by Fetter, Alexander L.; Walecka, John Dirk. San Francisco, McGraw-Hill [c1971]. International series in pure and applied physics, 1971).
- [10] J. Kapusta and T. Toimela, *Phys. Rev. D* **37**, 3731 (1988).
- [11] J. M. Ziman, *Principles of the theory of solids* (Principles of the theory of solids, by Ziman J.M. Cambridge, Cambridge University Press[c1972]., 1972).
- [12] B. Jancovici, *Il Nuovo Cimento* (1955-1965) **25**, 428 (1962).
- [13] V. A. Urpin and D. G. Yakovlev, *Sov. Astron.* **24**, 425 (1980).